Supplementary Information

A novel layered Cu-based perovskite metal-organic framework with 1,2-diaminoethane cations: synthesis, crystal structure, thermal and magnetic properties

Asmae Ben Abdelhadi[a,b], Rachid Ouarsal[a], Morgane Poupon[c], Michal Dusek[c], Juan Pedro Andrés González[d], Luis Lezama[e], Brahim El Bali[f], Mohammed Lachkar[a,*], and Abderrazzak Douhal[b,*]

[a]Engineering Laboratory of Organometallic, Molecular Materials, and Environment (LIMOME), Faculty of Sciences, Sidi Mohamed Ben Abdellah University, 30000 Fez, Morocco.

[b]Departamento de Química Física, Facultad de Ciencias Ambientales y Bioquímica, y INAMOL, Campus Tecnológico de Toledo, Universidad de Castilla-La Mancha (UCLM), Avenida Carlos III, S.N., 45071 Toledo, Spain.

[c]Institute of Physics of the Czech Academy of Sciences, Na Slovance 2, 8, Praha 182 21, Czech Republic.

[d]Departamento de Física Aplicada, Instituto Regional de Investigación Científica Aplicada (IRICA), Universidad de Castilla - La Mancha, 13071, Ciudad Real, Spain.

[e]Departamento de Química Orgánica e Inorgánica, Facultad de Ciencia y Tecnología, Universidad del País Vasco, UPV/EHU, Bº Sarriena s/n, 48940 Leioa, Spain.

[f]Independent Scientist, Marrakech, Morocco.

*Corresponding authors: mohammed.lachkar@usmba.ac.ma and abderrazzak.douhal@uclm.es

Index

Single crystal X-ray measurements

For the X-ray diffraction experiments, we used on a blue rectangular single crystal block 0.69 × 0.48 × 0.45 mm^3. Data collection was performed using Mo Kα radiation (λ = 0.71073Å) from a classical sealed tube monochromated by graphite and collimated by fibre-optics Enhance collimator. We used as a detector, a CCD detector Atlas S2, CrysAlis PRO software (CrysAlis PRO 1.171.41.117a, Rigaku Oxford Diffraction, 2021);)to process the data and an empirical multiscan absorption correction was applied using spherical harmonics, implemented in the SCALE3 ABSPACK scaling algorithm. The structure was solved by charge flipping with the program SUPERFLIP package[1] and refined against F^2 by using full-matrix least-squares methods with the Jana2020 program package.[2] Hydrogen atoms were found using the Fourier difference map, the hydrogens of the ethylene diammonium carbons were placed in calculated positions and were refined as riding atoms. The hydrogens on the carbons of the formate ion and on the nitrogen of the ethylenediammonium cation were placed using the Fourier map difference and their positions have been refined. All non-hydrogen atoms were refined with anisotropic thermal displacement parameters. For all the hydrogen atoms, we kept U_{iso}(H) equal to 1.2Ueq(C/N). Visualization of the structure was made using the diamond program.[3]

Table S1. Fractional atomic coordinates and isotropic or equivalent isotropic displacement parameters (Å^2) for **1.**

	x	*y*	*z*	U_{iso}*/U_{eq}
Cu1	0	0.5	0.5	0.01471 (12)
O1	−0.10540 (13)	0.35078 (17)	0.61811 (13)	0.0210 (4)
O2	0.20924 (14)	0.29091 (18)	0.57865 (15)	0.0284 (5)
O3	0.10633 (13)	0.66325 (17)	0.68326 (13)	0.0215 (4)
O4	0.34945 (16)	0.01999 (18)	0.62240 (19)	0.0310 (5)
N1	0.40405 (18)	0.6094 (3)	0.62937 (18)	0.0234 (6)
C1	0.23065 (19)	0.1085 (3)	0.5758 (2)	0.0241 (6)
C2	0.4626 (2)	0.5994 (3)	0.4994 (2)	0.0263 (7)
C3	0.04285 (18)	0.7523 (3)	0.76281 (19)	0.0175 (6)
H1C2	0.531077	0.706071	0.508492	0.0316*
H2C2	0.38456	0.614219	0.403768	0.0316*
H1N1	0.471 (2)	0.590 (3)	0.718 (2)	0.0281*
H2N1	0.361 (2)	0.726 (3)	0.631 (2)	0.0281*
H3N1	0.348 (3)	0.500 (3)	0.628 (3)	0.0281*
H1C1	0.146176	0.026216	0.532922	0.0289*
H1C3	−0.063 (2)	0.744 (3)	0.727 (2)	0.021*

Table S2. Atomic displacement parameters (Å^2) for **1**.

	U^{11}	U^{22}	U^{33}	U^{12}	U^{13}	U^{23}
Cu1	0.01940 (19)	0.01421 (18)	0.01200 (18)	−0.00242 (10)	0.00714 (13)	−0.00069 (10)
O1	0.0205 (6)	0.0242 (7)	0.0183 (6)	−0.0015 (5)	0.0064 (5)	0.0068 (5)
O2	0.0250 (7)	0.0185 (7)	0.0423 (8)	0.0017 (5)	0.0118 (6)	0.0010 (6)
O3	0.0221 (6)	0.0241 (7)	0.0205 (6)	−0.0021 (5)	0.0101 (5)	−0.0083 (5)
O4	0.0262 (7)	0.0230 (7)	0.0385 (9)	0.0057 (5)	0.0032 (7)	0.0007 (5)
N1	0.0209 (8)	0.0213 (9)	0.0282 (9)	0.0036 (7)	0.0081 (7)	−0.0008 (7)
C1	0.0222 (9)	0.0214 (10)	0.0265 (10)	−0.0031 (7)	0.0048 (8)	0.0002 (8)
C2	0.0286 (10)	0.0217 (10)	0.0331 (11)	0.0052 (8)	0.0161 (9)	0.0035 (8)
C3	0.0190 (8)	0.0166 (8)	0.0175 (9)	0.0003 (6)	0.0067 (7)	0.0011 (7)

Table S3. Selected bond distances (Å) and angles (°) for **1**.

Cu1—O1i	1.9831 (13)	N1—C2	1.479 (3)
Cu1—O2	2.3787 (12)	N1—H1N1	0.868 (19)
Cu1—O2i	2.3787 (12)	N1—H2N1	0.89 (2)
Cu1—O3	1.9880 (11)	N1—H3N1	0.91 (2)
Cu1—O3i	1.9880 (11)	C1—H1C1	0.96
O1—C3ii	1.2500 (19)	C2—C2iii	1.513 (3)
O2—C1	1.238 (2)	C2—H1C2	0.96
O3—C3	1.248 (2)	C2—H2C2	0.96
O4—C1	1.243 (2)	C3—H1C3	0.978 (19)
O1—Cu1—O1i	180	C2—N1—H1N1	111.9 (17)
O1—Cu1—O2	94.69 (5)	C2—N1—H2N1	110.7 (15)
O1—Cu1—O2i	85.31 (5)	C2—N1—H3N1	109.7 (18)
O1—Cu1—O3	91.96 (5)	H1N1—N1—H2N1	109.4 (19)
O1—Cu1—O3i	88.04 (5)	H1N1—N1—H3N1	99 (2)
O1i—Cu1—O2	85.31 (5)	H2N1—N1—H3N1	115 (2)
O1i—Cu1—O2i	94.69 (5)	O2—C1—O4	127.20 (16)
O1i—Cu1—O3	88.04 (5)	O2—C1—H1C1	116.4
O1i—Cu1—O3i	91.96 (5)	O4—C1—H1C1	116.4
O2—Cu1—O2i	180	N1—C2—C2iii	110.04 (16)
O2—Cu1—O3	84.65 (4)	N1—C2—H1C2	109.47
O2—Cu1—O3i	95.35 (4)	N1—C2—H2C2	109.47
O2i—Cu1—O3	95.35 (4)	C2iii—C2—H1C2	109.47
O2i—Cu1—O3i	84.65 (4)	C2iii—C2—H2C2	109.47
O3—Cu1—O3i	180	H1C2—C2—H2C2	108.9
Cu1—O1—C3ii	123.33 (12)	O1iv—C3—O3	124.60 (16)
Cu1—O2—C1	134.82 (11)	O1iv—C3—H1C3	119.0 (12)
Cu1—O3—C3	122.32 (10)	O3—C3—H1C3	116.4 (12)

Symmetry codes: (i) −x, −y+1, −z+1; (ii) −x, y−1/2, −z+3/2; (iii) −x+1, −y+1, −z+1; (iv) −x, y+1/2, −z+3/2.

Characteristic vibrations of formate anion.

The strongest characteristic formate vibrations bands are as follows: the absorption band at 1557 cm^{-1} corresponds to the C–O asymmetric stretching modes ν_4(HCOO), and the C-H in-plane bending mode ν_5(HCOO) of formate group is observed as an intense band at 1370 cm^{-1}. The C-O symmetric stretching mode ν_2(HCOO) exhibits strong absorption bands at 1357 and 1343 cm^{-1}, while the out-of-plane C–H bending mode ν_6(HCOO) vibration is observed at 1070 cm^{-1}. The absorption bands at 823 and 763 cm^{-1} can be associated to the symmetric O-C-O bending mode ν_3(HCOO).[42] It is also worth noticing the split of this last deformation band since the structure includes two types of $HCOO^-$, apical-terminal and equatorial-bridging ones (Figure 2 and Table S4).

Table S4. The assignment of the IR bands at room temperature. The abbreviations are as follows (s: strong, vs: very strong, m: medium, w: weak, vw: very weak, sh: shoulder).

$(NH_3(CH_2)_2NH_3)[Cu(HCO_2)_4]$	
Wavenumber (cm^{-1})	Assignement
3311 m, 3255 m, 3157 m and 3027 sh	N−H, stretching
2962 sh	$2\nu_4$
2896 m and 2817 m	C−H stretching, ν_1
2711 w	$2\nu_5$
2574 vw,2439 w and 2158 vw	Combination
1720 w	N−H bending
1629 vs and 1557 vs	δasNH_3^+ and COO, stretching, antisym., ν_4
1423 sh	C−H_2 bending
1370 vs and 1343 s	δCH and COO deformation, antisym., ν_5
1157 w and 1114 m	rocking NH_3
1076 vw	C−H, out of plane deformation, ν_6
1056 w	νCC
1020 w	νCN
823 m and 805 vw	ρNH_3^+
763 w	COO deformation, sym., ν_3
545 w	δCC

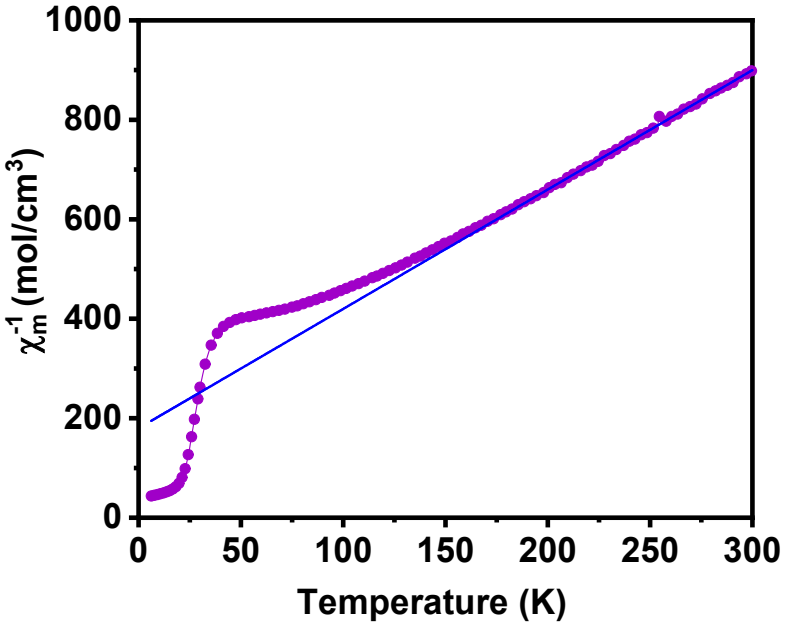

Figure S1. Thermal evolution of the reciprocal molar magnetic susceptibility of compound **1** measured at 10 kOe. The continuous line represents the Curie-Weiss fit (see text for the details).

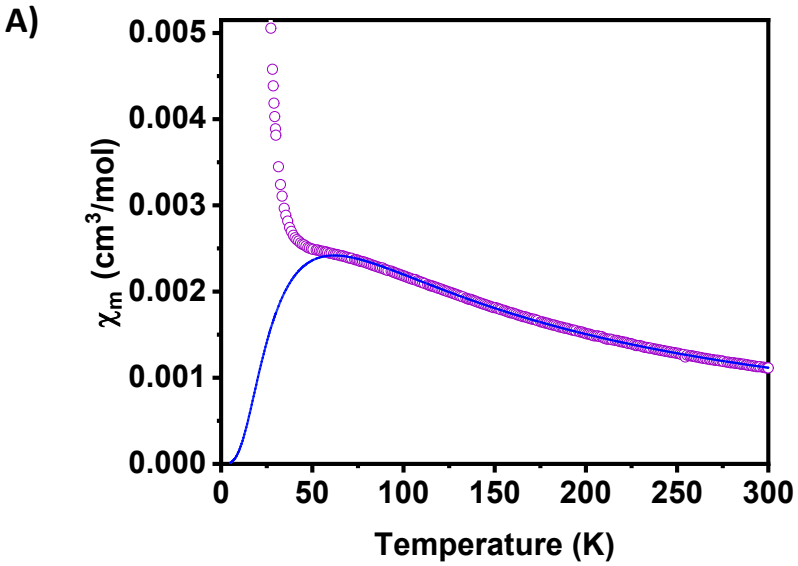

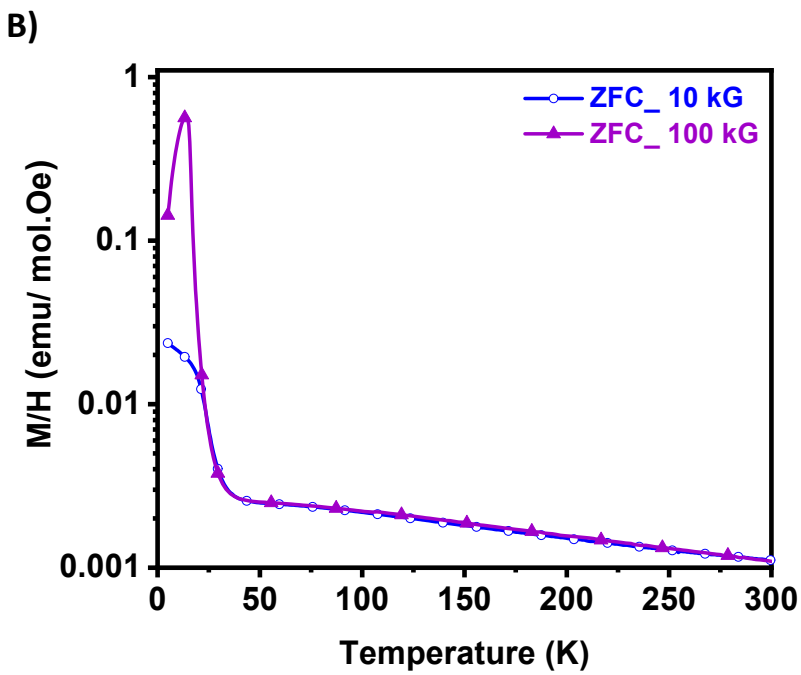

Figure S2. Thermal evolution of the molar magnetic susceptibility of compound **1** measured at 10 kOe. The continuous line represents the best fit obtained for the high-temperature data to a 2D antiferromagnetic model (see text for the details) (A). M/H vs temperature curves obtained between 5 and 300 K under applied fields of 100 Oe and 10 kOe (B).

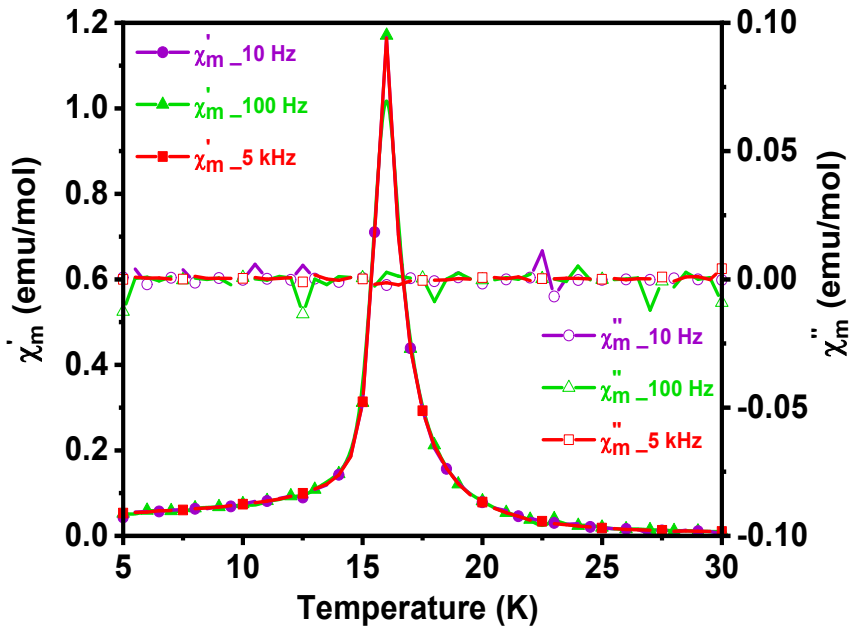

Figure S3. AC magnetic susceptibility measurements for **1** in zero applied field.

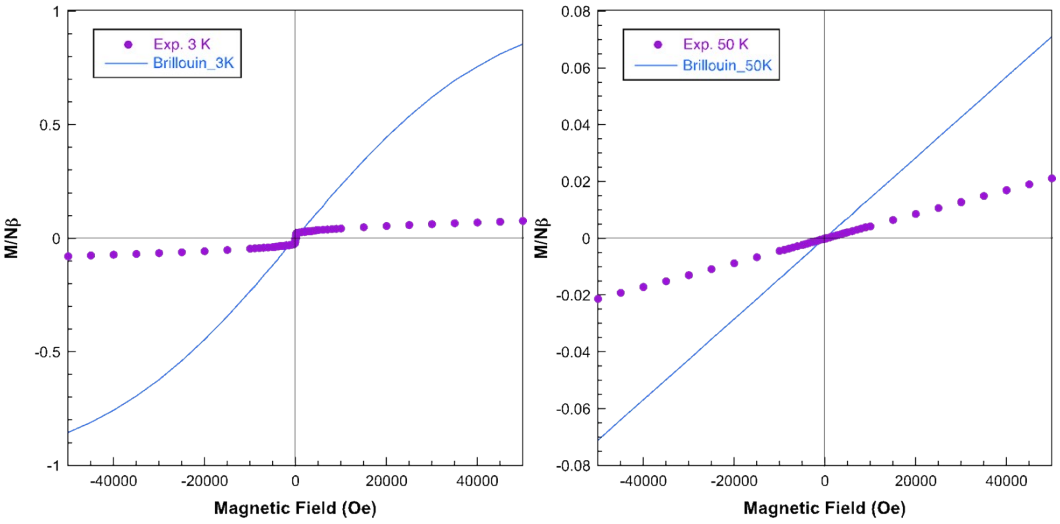

Figure S4. Magnetization curves for compound **1** at 3 K (left) and 50 K (right).

Acknowledgements

This work is also supported by the following grants: PID2020-116519RB-I00 funded by MCIN/AEI/10.13039/501100011033 and the European Union (EU) and the EU through "Fondo Europeo de Desarrollo Regional" (FEDER): 2022-GRIN-343259 and 2022-GRIN-34313 funded by UCLM (FEDER, EU). A.B.A. thanks the grant from the Spanish Service for the Internationalization of Education (SEPIE) for her stay at the UCLM, through the EU Erasmus+ key action program (2020-1-ES01-KA107-079868). We thank the technical assistance of Interface Regional University Center at the University Sidi Mohammed Ben Abdellah (USMBA, Fez, Morocco), and the USMBA for the financial support.

References

1. L. Palatinus and G. Chapuis, *J. Appl. Cryst.*, 2007, **40**, 786-790.
2. V. Petříček, L. Palatinus, J. Plášil and M. Dušek, *Z Kristallogr Cryst Mater*, 2023, **238**, 271-282.
3. K. Brandenburg and H. Putz, *Crystal Impact GbR, Bonn, Germany*, 2006.